Coherent reflection of light from a turbid suspension of particles in an internal-reflection configuration: Theory versus experiment

Augusto García-Valenzuela[1†], Rubén G. Barrera[2*], Celia Sánchez-Pérez[1], Alejandro Reyes-Coronado[2], and Eugenio R. Méndez[3]

[1] *Centro de Ciencias Aplicadas y Desarrollo Tecnológico, Universidad Nacional Autónoma de México. Apartado Postal 70-186, 04510 México D.F., México*
[2] *Instituto de Física, Universidad Nacional Autónoma de México Apartado Postal 20-364, 01000 México D.F., México.*
[3] *División de Física Aplicada, Centro de Investigación Científica y Estudios Superiores de Ensenada, Apartado Postal 2732, 22860 Ensenada Baja California, México.*
**Consultant at Centro de Investigación en Polímeros, COMEX, México.*
†garciaa@aleph.cinstrum.unam.mx

Abstract: We compare a recently developed coherent-scattering model for the reflectance of light from a turbid colloidal suspension of particles with experimental measurements. The experimental data were obtained in an internal reflection configuration around the critical angle using a glass prism in contact with a monodisperse colloidal suspension of latex particles, and a polydisperse suspension of TiO2 particles. First, we review the coherent scattering model and extend it to the case of polydisperse suspensions in an internal reflection configuration. The experimental data is then compared with results of the coherent scattering model and results obtained assuming that the colloidal system can be treated as a homogeneous medium with an effective index of refraction. We find that the experimental results are not compatible with the effective medium model. On the other hand, good fits to the experimental curves can be obtained with the coherent scattering model.

OCIS codes: (290.5850) Scattering, particles; (030.1670) Coherent optical effects; (290.7050) Turbid media; (290.4210) Multiple scattering; (160.4760) Optical properties; (120.5700)

References

1. M Lax, "Multiple scattering of waves II. The effective field in dense systems" Phys. Rev. **85** 621 (1952).
2. L Tsang and J A Kong, *Scattering of electromagnetic waves: Advanced topics* (Wiley, New York, 2001).
3. L Tsang and J A Kong, "Effective propagation constants for coherent electromagnetic waves propagating in media embedded with dielectric scatterers" J. Appl. Phys. **53**, 7162 (1982).
4. A García-Valenzuela and R G Barrera, "Electromagnetic response of a random half-space of Mie scatterers within the effective medium approximation and the determination of the effective optical coefficients" J. Quant. Spectrosc. Radiat. Transfer **627**, 79 (2003).
5. Y Kuga, D Rice and R D West, "Propagation constant and the velocity of the coherent wave in a dense strongly scattering medium" IEEE Trans. Antennas Propag. **44** (3), 326 (1996).
6. C Yang, A Wax and M S Feld, "Measurement of the anomalous phase velocity of ballistic light in a random medium by use of a novel interferometer" Opt. Lett. **26** (4), 235 (2001).
7. R G Barrera and A Garcia-Valenzuela, "Coherent reflectance in a system of random Mie scatterers and its relation to the effective-medium approach" J. Opt. Soc. Am. A **20** (2), 296 (2003).
8. A Garcia-Valenzuela and R G Barrera, "Optical reflectance of a composite medium with a sparse concentration of large spherical inclusions" Phys. Status Solidi B **240**, 480 (2003).
9. R G Barrera and A Garcia-Valenzuela, "Amperian magnetism in the dynamic response of granular materials", *Developments in Mathematical and Experimental Physics, Volume B: Statistical Physics and Beyond*, Edited by Macias *et al*. (Kluwer Academic, Plenum Publishers, 2003) pp. 147-170.

#8123 - $15.00 USD Received 15 July 2005; revised 15 August 2005; accepted 16 August 2005

10. A Garcia-Valenzuela, C Sánchez-Pérez, A Reyes-Coronado, R G Barrera, "Optical Characterization of a turbid colloid by light reflection around the critical angle" *Materials Science and Applied Physics, 2nd Mexican Meeting on Mathematical and Experimental Physics*, Eds. J L Hernández-Pozos, R Olayo-González, AIP Conference Proceedings **759**, 62 (2005).
11. C F Bohren, "Applicability of effective medium theories to problems of scattering and absorption by non-homogeneous atmospheric particles" J. Atmos. Sci. **43**, 468 (1986).
12. R Ruppin, "Evaluation of extended Maxwell Garnett theories" Opt. Commun. **182**, 273 (2000).
13. C F Bohren and D R Huffman, *Absorption and Scattering of Light by Small Particles* (J. Wiley & Sons, New York, 1983).
14. H C van de Hulst, *Light scattering by small particles* (Wiley, New York, 1957).
15. A Chou and M Kerker, "The refractive index of colloidal sols" J. Phys. Chem. **60**, 562 (1956).
16. J V Champion, G H Meeten and M Senior, "Refractive index of particles in the colloidal state" J. Chem. Soc., Faraday Trans. **74**, 1319 (1978).
17. K Alexander, A Killey, G H Meeten and M Senior, "Refractive index of concentrated colloidal dispersions" J. Chem. Soc. Farday Trans. **77**, 361 (1981).
18. G H Meeten and A N North , "Refractive index measurement of turbid colloidal fluids by transmission near the critical angle" Meas. Sci. Technol. **2**, 441 (1991).
19. G H Meeten and A N North , "Refractive index measurement of absorbing and turbid fluids by reflection near the critical angle" Meas. Sci. Technol. **6**, 214 (1995).
20. M Mohammadi, "Colloidal refractometry: meaning and measurement of refractive index for dispersions; the science that time forgot" Adv. Colloid & Interf. Sci. **62**, 17 (1995).
21. G H Meeten, "Refraction by spherical particles in the intermediate scattering region" Opt. Comm. **134**, 233 (1997).
22. G H Meeten, "Refractive index errors in the critical-angle and the Brewster-angle methods applied to absorbing and heterogeneous materials" Meas. Sci. Technol. **8**, 728 (1997).
23. Y Sarov, I Capek, S Janíčková, I Kostič, A Konečníková, L Matay, V Sarova, "Properties of nano-scaled disperse media investigated by refractometric measurements" Vacuum **76**, 231 (2004).
24. H Ding, J Q Lu, K M Jacobs, X-H Hu, "Determination of refractive indices of porcine skin tissues and intralipid at eight wavelengths between 325 and 1557 nm", J. Opt. Soc. Am. A **22** (6), 1151 (2005).
25. A Garcia-Valenzuela, C Sánchez-Pérez, R G Barrera, A Reyes-Coronado, "Surface effects on the coherent reflection of light from a polydisperse colloid", to be submitted.
26. F Curiel, *Predicción de propiedades ópticas de películas inhomogéneas por medio de modelos de transferencia radiativa y su aplicación en pinturas*, Ph.D. Thesis (Instituto de Física, Universidad Nacional Autónoma de México, México D.F. (2004).

1. Introduction

When light, traveling in a transparent homogeneous medium, strikes the flat interface of a medium with random inhomogeneities, scattered light appears on both sides of the boundary. The total intensity (I_T) can be separated, in general, as the sum of a coherent (I_c) or direct component, and a diffuse (I_d) or incoherent one. Defining the coherent intensity as the magnitude squared of the mean field, $I_c = |\langle E \rangle|^2$, the diffuse intensity is given by $I_d = \langle I_T \rangle - I_c$, where the angled brackets indicate an average over an ensemble of realizations of the random inhomogeneous medium. The fraction of the original power that goes into the diffuse component depends on the turbidity of the sample and the angle of incidence. A medium is regarded as homogeneous when the diffuse component is negligible, whereas a medium is considered turbid when the diffuse component can be easily detected. In homogeneous media the coherent or mean field coincides with the macroscopic field.

At a flat interface with a turbid medium, the mean field is refracted at the interface and propagates in the random medium in a manner that is consistent with the propagation of light in an equivalent homogeneous medium [1-10]. It is thus tempting to associate an effective index of refraction to the inhomogeneous medium and try to describe its optical properties (as far as the coherent field is concerned) in terms of this parameter [7-24]. While this is adequate for the case of small particles or inhomogeneities, it has been shown theoretically that for large ones the amplitudes of the reflected and transmitted mean fields are not consistent with those that can be calculated assuming this effective index of refraction in the usual Fresnel relations [7,8,11,13,19,20]. By large we mean particles with a size parameter, $x = 2\pi a/\lambda$, comparable or larger than one. Here a is the particles' radii and λ is the wavelength of the incident radiation in the medium surrounding the particles.

#8123 - $15.00 USD Received 15 July 2005; revised 15 August 2005; accepted 16 August 2005

The coherent reflectance of a dilute system of large particles is in general small. If the particles are embedded in a homogenous matrix material, the reflectance from the matrix interface will normally be much larger than that from the particles, making it difficult to evaluate the contribution from the particles. An important exception occurs close to the critical angle in an internal-reflection configuration. The optical reflectance near the critical angle is highly sensitive to the optical properties of the external media. Not surprisingly, critical-angle refractometry has been used for the determination of the effective refractive index of turbid colloids [15-24]. Some evidence of inconsistencies arising from assuming valid the use of the effective refractive index in the Fresnel relations to calculate the reflectivity of light from a turbid colloid when particles are large was found in the experimental work of Meeten and North in Ref. [19]. The present paper is motivated in part by the need to provide further experimental evidence on this matter.

From the theoretical studies, it is apparent that the reflectivity of a sample will depend on several parameters of the medium, like the density of particles, their refractive indices and size distribution. It is thus natural to think that some of these quantities can be inferred from reflectivity measurements. To solve this inverse problem, however, it is necessary to have simple and reliable solutions to the direct problem. The coherent reflection of light from an ensemble of randomly placed particles can be obtained theoretically by setting up a system of equations for the exciting fields at each particle, solving the coupled multiple-scattering equations for the electromagnetic fields, and taking a configurational average. For a random system of particles it is possible to obtain a hierarchy of equations using, at each level in the hierarchy, more detailed statistical information about the system than in the level below. For instance, at the first level one requires only the number density of particles. At the second level besides the number density one requires the two-particle correlation function. At the third level, besides these two functions, one requires the three-particle correlation function, and so on [2,3]. Truncation at the first stage in the hierarchy yields to the so-called "effective-field approximation" and is limited to a dilute system of particles. In this approximation the coherent reflection coefficient of a monodisperse system of particles was derived in Ref. [4]. At the second stage in the hierarchy, the resulting approximation is known as the "quasi-crystalline approximation" which is appropriate for denser systems. Using this approximation Kong and collaborators [2,3] devised a calculation procedure for the coherent reflection amplitude from a half space of randomly-located spherical particles. Both of these approximations are valid for small as well as for large particles.

Although calculations with the quasi-crystalline approximation or even more sophisticated approximations are possible with modern computers, considering the time required for these calculations, it is clear that in practice they can not be used to implement a fitting routine for experimental data analysis. In a recent paper [7] a more intuitive approach to calculate the coherent reflection from a dilute half-space of randomly located identical particles was used. Basically, in this model the system is regarded as a collection of thin slabs; the multiple-scattering equations for the coherent wave among the slabs are then solved yielding to closed expressions for the coherent reflection coefficients. From now on we will refer to this model as the coherent-scattering model (CSM).

The coherent-scattering model is, to our knowledge, the only available candidate at present to be used for routine experimental data analysis in order to characterize particles in suspension in optically turbid media. Thus, the main purpose of this work is to test its validity against experimental data. In doing so, we also corroborate the inconsistencies of an effective medium model in the case of large colloidal particles. We provide experimental results for suspensions of monodisperse latex particles and polydisperse TiO_2 (rutile) particles, both dispersed in water, with different densities.

The paper is organized as follows. First, in section 2 we present a summary of the coherent-scattering model and extend it to consider the coherent reflection from a half-space of a polydisperse, random system of particles in an internal reflection configuration. In section 3 we describe our experimental setup and methods. We present experimental results for suspensions of monodisperse latex particles in water and polydisperse TiO_2 (rutile) particles

#8123 - $15.00 USD Received 15 July 2005; revised 15 August 2005; accepted 16 August 2005

in water with different densities. In section 4 we present a comparison of the theoretical and experimental results, together with a discussion. Finally, in section 5 we deliver our conclusions.

2. Coherent-scattering model

The model we consider in this paper uses scattering theory for the calculation of the coherent reflectance from a half-space of a random medium, and it was originally derived in Ref. [7]. There, one considered the case of a dilute monodisperse system of randomly located spherical particles. Here, we summarize the main results obtained in Ref. [7] and provide their extension to the case of a polydisperse system of spherical particles and discuss their use in an internal reflection configuration. As already said, we will refer to this model as the coherent-scattering model (CSM).

2.1 Coherent reflection coefficient from a polydisperse random system of particles

The derivation of the coherent-scattering model in Ref. [7] is based on the slicing of the half-space containing the particles into thin slabs as shown in Fig. 1a. First, for a thin slab, the coherent reflected and transmitted wave is calculated in the single-scattering approximation. Then, the reflection coefficient of the half-space is obtained by taking account of the multiple scattering of the coherent wave between the semi-infinite pile of slabs. These calculations are done assuming that the thickness of each slab is small compared to the wavelength of radiation, and there is no correlation between the positions of the particles, that is, the exclusion volume is ignored. The approximations used in this derivation of the half-space reflection coefficient limit its validity to dilute systems of particles, but it can be used for large particles. By large particles we mean particles with size parameter comparable or larger than one.

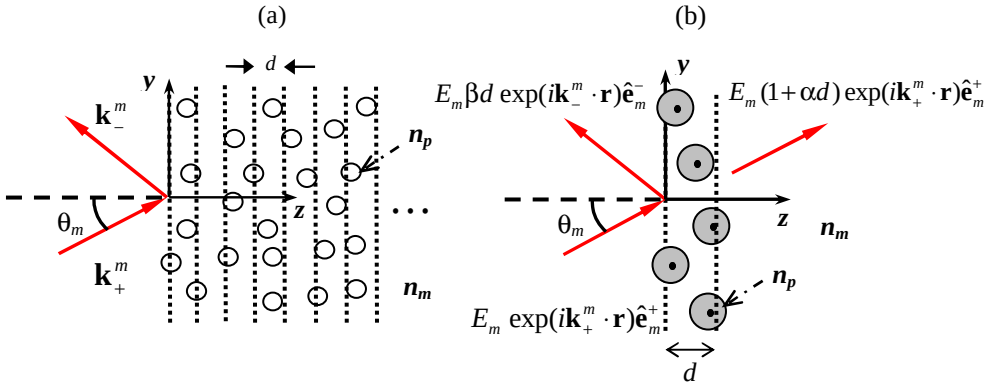

Fig. 1. Coherent reflection and transmission of light from a random system of particles. a) Half-space formed by a semi-infinite pile of thin slabs, and b) coherent reflection and transmission from an isolated thin slab.

The results obtained in Ref. [7] may be summarized as follows: Consider a plane wave, $\mathbf{E}^m = E_m \exp(\mathbf{k}_+^m \cdot \mathbf{r})\,\hat{\mathbf{e}}_m^+$, is incident into a thin slab of spherical particles of radii a embedded in a boundless homogeneous medium (the matrix) with their centers located at random between the planes $z = 0$ and $z = d$ as shown in Fig. 1b. The coherent scattered waves to the right and left of the slab are given by [7],

$$\left\langle \mathbf{E}^S \right\rangle = E_m \begin{cases} \alpha d \exp(i\mathbf{k}_+^m \cdot \mathbf{r})\hat{\mathbf{e}}_m^+ & \text{for } z > d \\ \beta d \operatorname{sinc}(k_z^m d) \exp(i\mathbf{k}_-^m \cdot \mathbf{r})\hat{\mathbf{e}}_m^- & \text{for } z < 0 \end{cases}, \qquad (1)$$

where

#8123 - $15.00 USD Received 15 July 2005; revised 15 August 2005; accepted 16 August 2005

$$\alpha = -\frac{2\pi\rho}{k_m^2 \cos\theta_m} S(0), \qquad \beta = -\frac{2\pi\rho}{k_m^2 \cos\theta_m} S_j(\pi - 2\theta_m). \tag{2}$$

In the above expressions, E_m is the amplitude of the incident wave, d is the width of the slab, $\mathbf{k}_+^m$ and $\mathbf{k}_-^m$, and $\hat{\mathbf{e}}_m^+$ and $\hat{\mathbf{e}}_m^-$ are the wavevectors and polarization vectors of the incident and the coherent reflected wave, respectively, ρ is the number density of particles, $k_m = n_m k_0$ is the wave number of the incident wave, n_m is the refractive index of the medium surrounding the particles (the matrix), θ_m is the angle of incidence, and $k_0 = 2\pi / \lambda_0$ is the wave number in vacuum. The functions $S_j(\theta_S)$ are the diagonal components of the 2×2 amplitude scattering matrix of an isolated spherical particle embedded within the matrix material, as defined in Ref. [14]. Here θ_S is the scattering angle and $j = 1$ corresponds to a TE and $j = 2$ to a TM polarized incident wave, respectively. For a sphere, the forward scattering amplitude $S_1(\theta = 0) = S_2(\theta = 0) \equiv S(0)$. In the geometry shown in Fig. 1, we have that, $\mathbf{k}_+^m = k_m \sin\theta_m \hat{\mathbf{a}}_y + k_m \cos\theta_m \hat{\mathbf{a}}_z$, $\mathbf{k}_-^m = k_m \sin\theta_m \hat{\mathbf{a}}_y - k_m \cos\theta_m \hat{\mathbf{a}}_z$, $\hat{\mathbf{e}}_m^+ = \hat{\mathbf{e}}_m^- = \hat{\mathbf{a}}_x$ for a TE polarized incident wave, while for a TM polarized incident wave $\hat{\mathbf{e}}_m^+ = \cos\theta_m \hat{\mathbf{a}}_y - \sin\theta_m \hat{\mathbf{a}}_z$, $\hat{\mathbf{e}}_m^- = -\cos\theta_m \hat{\mathbf{a}}_y - \sin\theta_m \hat{\mathbf{a}}_z$.

With this notation, the coherent reflection coefficient, r_{hs}, of the half-space of randomly located spheres, obtained in Ref. [7], can be written as

$$r_{hs} = \frac{\beta}{i(k_z^{eff} + k_z^m) + \alpha}, \tag{3}$$

where

$$k_z^{eff} = \sqrt{(k_z^m)^2 - 2i\alpha k_z^m + \beta^2 - \alpha^2}, \tag{4}$$

$k_z^m = k_m \cos\theta_m$ is the z-component of the incident wavevector, and k_z^{eff} may be regarded as the z-component of an effective wavevector. Although we use the term "effective" to denote the wavevector of the coherent wave, this does not mean the results in Eq. (3) and (4) are based on an effective medium approach. They are obtained from scattering theory. Now, considering that the y-component of the effective wavevector must be equal to that of the incident wavevector and that $\left(k_z^{eff}\right)^2 + \left(k_y^{eff}\right)^2 = \left(\tilde{n}_{eff} k_0\right)^2$, we obtain an expression for the effective refractive index as, $\tilde{n}_{eff} = \left[n_m{}^2 - 2i\,\alpha(k_z^m / k_0^2) + (\beta^2 - \alpha^2)/k_0^2 \right]^{1/2}$. If we drop the second order terms, $\beta^2 - \alpha^2$, we obtain the so called van de Hulst effective refractive index [14],

$$\tilde{n}_{eff} \simeq n_m \left(1 + i \frac{2\pi}{k_m^3} \rho S(0) \right). \tag{5}$$

These results correspond to a monodisperse system of spherical particles of radius a embedded in a boundless homogenous matrix. It is assumed that the center of all particles lie in the half-space $z > 0$.

Now, for a polydisperse system of particles, the number density of particles is a function of the particles radius: $\rho(a)$. To extend the above results to a polydisperse system of particles we must average the scattering coefficients of a thin slab, α and β, with respect to the particle size. These coefficients are calculated in the single scattering approximation and averaging them is straight forward. It consists of replacing in α and β the elements of the amplitude scattering matrix by the integral with respect to the radii of the product of $\rho(a)$ times the

#8123 - $15.00 USD Received 15 July 2005; revised 15 August 2005; accepted 16 August 2005

corresponding element of the amplitude scattering-matrix associated to radius a. Therefore, for a polydisperse system of spheres we have,

$$\alpha = -\frac{2\pi}{k_m^2 \cos\theta_m}\int_0^\infty \rho(a) S_a(0) da \,,$$

$$\beta = -\frac{2\pi}{k_m^2 \cos\theta_m}\int_0^\infty \rho(a) S_{a,j}(\pi - 2\theta_m) da \,. \qquad (6)$$

The subscript a in the S functions is used to remark its dependence on the radius of the particles. The number density of particles $\rho(a)$ may be written as $\rho_T n(a)$, where ρ_T is the total number density of particles, regardless of their radius, and $n(a)$ is the so called size distribution function. It is common to find that $n(a)$ follows a log-normal distribution function,

$$n(a) = \frac{1}{a\sqrt{2\pi}\ln\sigma}\exp\left(-\frac{\ln^2(a/a_0)}{2\ln^2\sigma}\right), \qquad (7)$$

where a_0 is the most probable radius, and σ is the width parameter of the distribution. In the experiments, however, the control is over the volume fraction occupied by the spheres, f, rather than over the total number of particles per unit volume, ρ_T. Thus one should use ρ_T given by,

$$\rho_T = \frac{3f}{4\pi a_0^3}\exp\left[-\tfrac{1}{2}\left(3\ln\sigma\right)^2\right]. \qquad (8)$$

In conclusion, the half-space reflection coefficient from a half-space of a polydisperse system of particles embedded in a boundless homogeneous medium is calculated by Eqs. (3) and (4) with the scattering coefficients given in Eq. (6). The effective refractive index is now given by,

$$\tilde{n}_{eff} \approx n_m\left(1 + i\frac{2\pi}{k_m^3}\int_0^\infty \rho(a) S_a(0) da\right). \qquad (9)$$

2.2 Reflection coefficient with a matrix interface

The half-space reflection coefficient given in the previous section corresponds to a random system of spheres where the center of all particles lies in the half-space $z > 0$. The plane $z = 0$ may be regarded as a plane interface between the matrix medium and the composite matrix. At this point we may replace the composite medium by an artificial homogenous medium occupying the half-space $z > 0$ whose reflection coefficient is r_{hs}, as given in Eq. (3). In an actual experiment, we have an additional interface, namely, the incident-medium – matrix interface, as shown in Fig. 2. Let us assume that the incidence medium is non-absorbing with a refractive index n_1, and the interface with the matrix is at $z = 0$. The incident wave comes at an angle θ_i and is refracted upon transmission inside the matrix material. The angle of travel of light within the matrix, θ_m, is determined by Snell's law at the interface: $n_1\sin\theta_i = n_m\sin\theta_m$. Let us now displace the half-space of particles to the right by a distance $z_s > a_{max}$, where a_{max} is the maximum possible radii of the particles, or a value for which the probability of finding larger particles is negligible. In this way, the center of all the particles (or the great majority of them) lies to the right of the plane $z = z_s$, thus no particles crosses the plane $z = 0$, and the reflection coefficient of the half-space of particles at an angle of incidence θ_m, gains the phase factor: $\exp(2in_m k_0 \cos\theta_m z_s)$. Then, the compound reflection coefficient of the two interfaces becomes,

#8123 - $15.00 USD Received 15 July 2005; revised 15 August 2005; accepted 16 August 2005

$$r = \frac{r_{12}^{Fresnel} + r_{hs}(\theta_m)\exp(2in_m k_0 \cos\theta_m z_s)}{1 + r_{12}^{Fresnel} r_{hs}(\theta_m)\exp(2in_m k_0 \cos\theta_m z_s)}, \tag{10}$$

where

$$\theta_m = \arcsin\left(\frac{n_1}{n_m}\sin\theta_i\right), \tag{11}$$

and $r_{12}^{Fresnel}$ is the Fresnel reflection coefficient for the simple incident-medium – matrix interface.

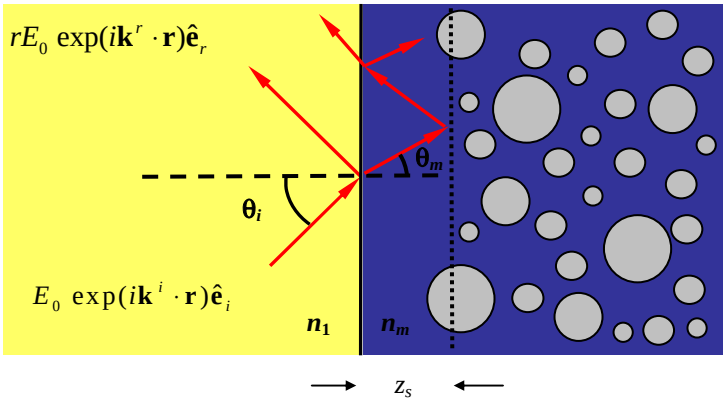

Fig. 2. Illustration of the reflection of the coherent wave from the compound interface: incident-medium − matrix and matrix − composite-matrix interface.

Now, if we consider a monodisperse system of spheres with radii a and assume there is no correlation among the positions of the spheres, but that there is an excluded-volume correlation between the spheres and the interface, then, any particle can approach the incident-medium – matrix interface up to $z = a$. In this case, we should use $z_s = a$ in Eq. (10). This result was already given in Ref. [7]. However, in the case of a polydisperse system of particles and under the same assumptions just described, an additional difficulty arises; namely, the size distribution function and volume fraction are modified near the interface because the center of a small particle can be closer to the interface than that of a large particle. If the incidence-medium interface is at $z = 0$, the size distribution function changes to

$$\rho(a, z) = U(z - a)\rho(a), \tag{12}$$

where U is the unit step function, that is, $U(x) = 0$ if $x < 0$ and $U(x) = 1$ if $x > 0$. The volume fraction becomes a function of z as well. The region of the smooth transition of $\rho(a, z)$ and $f(z)$ from zero at $z = 0$ to their bulk value at $z > a_{max}$ may be called the surface region. To retain the same level of approximation that our model has for a monodisperse system, we should model the half-space as a succession of thin slabs, but we must take into account that the slabs near the interface have a different size distribution function, $\rho(a, z)$. This can be done by dividing the whole system in a uniform half-space of constant f and $\rho(a)$, plus a finite number of slabs of variable $\rho(a, z)$ placed in front. To calculate the reflection coefficient of the whole system, one may start with the reflection coefficient of the uniform half-space and then add slabs in front, one by one, and calculate the reflection coefficient after each slab is added. This yields a well-defined iterative procedure for the calculation of the reflection coefficient. For simplicity, we will introduce here a new approximation and assume that all particles, regardless of their radius, are randomly distributed from $z = a_0$ to $z = \infty$. We will

#8123 - $15.00 USD Received 15 July 2005; revised 15 August 2005; accepted 16 August 2005

refer to this approximation as the "sharp surface" approximation. Therefore, in the sharp-surface approximation the coherent reflection coefficient is given by Eq. (10) with $z_s = a_0$, that is, the most probable radius. In this approximation we are ignoring that particles with a larger radius than a_0 remain farther away from the interface while smaller particles approach it closer. In fact, we have compared the results of calculating the reflection coefficient with the sharp-surface approximation with the ones obtained using the iterative procedure mentioned above, and found that both methods differ only for size distributions of width larger than the wavelength of the incident radiation [25]. The lower the contrast between the refractive index of the particles and the matrix, the more robust is the sharp surface approximation, being valid for wider size distributions [25]. In case of the experiments presented below, the curves predicted by the sharp surface approximation follow closely those obtained by the iterative procedure which takes detail account of the surface region. Thus here the sharp-surface approximation is used just to make the theoretical analysis as transparent as possible.

As we have already mentioned, our main objective in this paper is to test the coherent-scattering model by comparing it with experimental data in an internal-reflection configuration. We may note that in this case, when the angle of incidence is larger than the critical angle of the incident-medium – matrix interface, θ_m in Eq. (11), becomes complex. Therefore, the average field exciting the particles is actually an evanescent wave. This poses no problem to our formulation in terms of the elements of the amplitude scattering matrix because the mathematical procedure remains valid for an exciting field with a complex wavevector.

We are interested also in comparing the experimental data with a naïve application of the effective-medium concept. One may construct a simple effective-medium model by using Fresnel relations for an interface between the incident medium and an artificial homogeneous medium with an effective refractive index given by the van de Hulst formula. We will refer to this latter model as the isotropic effective-medium model (IEMM). Although this naïve application of the effective-medium concept has been proved to be incorrect in case of large colloidal particles [7-11], the IEEM has been used without restrain, for some time now, to interpret measurements of the "index of refraction" of colloids using critical angle refractometers [17-24]. For particles very small compared to the wavelength, r_{hs} in Eq. (3) and the IEMM predict similar values of the coherent reflectance for all angles of incidence. However, for particles with a size parameter that is not small compared to one, the coherent reflectance predicted by both models differs appreciably for both polarizations [7-11].

We should note that in our previous work [7-9], we dropped the second order terms $\beta^2 - \alpha^2$, in the expression for k_z^{eff} in Eq. (4) which is used in the expression for r_{hs} in Eq.(3). For angles of incidence not too close to grazing these terms contribute negligibly to the reflection coefficient for low density systems of particles. Near grazing angles they may contribute noticeably, although not strongly for dilute systems. However, in an internal reflection configuration, numerical evaluation of Eq. (3) shows that if these second order terms are dropped, the angle derivative of the reflectance becomes discontinuous at the critical angle of the incidence-medium – matrix interface, that is, at $\theta_i = \sin^{-1}(n_m / n_1)$. The discontinuity increases as the particle radii increases. This indicates that these terms are important near the critical angle in an internal-reflection configuration and must be kept in our model.

In the next section we compare the coherent-scattering model with experimental data in an internal-reflection configuration and around the critical angle. In calculating the theoretical curves with the coherent-scattering model we used the "sharp surface" approximation for the cases of polydisperse systems of particles, and we included the second order terms in the expression for k_z^{eff} in Eq. (4).

#8123 - $15.00 USD Received 15 July 2005; revised 15 August 2005; accepted 16 August 2005

3. Experimental setup and methods

The objective of our experiments is to obtain reliable experimental data of the coherent reflectance of a well collimated beam from a glass-colloid interface and compare it with the coherent-scattering model described in the previous section. As already explained, the coherent component of the reflected light corresponds to the average of the reflected electromagnetic fields over all possible configurations of the random system. In experiments, however, one measures the light power which has, in addition to the coherent component, a contribution from the diffuse light. The reason is that although the average of the diffuse electromagnetic fields is zero, the average of the diffuse optical power is not. When a well collimated light beam is incident to the interface of a turbid medium, the coherently reflected beam travels along the specular direction, whereas the diffuse light is normally distributed over a broad range of reflection angles. This experimental fact can be used to separate these two contributions in the measurements. The reflectivity of the sample can be estimated by baffling or spatial filtering the light in the specular direction. Inevitably, however, some diffuse light will be captured as well and, to correct for this, one must estimate the contribution of the diffuse light and subtract it from the measurement. Since the diffuse component normally consists of a broad, rather featureless distribution, a simple way of doing this is to measure the light power received by the detector in near-specular directions.

The experimental setup is shown in Fig. 3. A collimated beam of light (λ=6350 nm), coming from a laser diode of circular cross-section (approximately 3 mm in diameter) is incident on a glass (BK7) Dove prism. The sample is contained in the cavity formed by clamping an O-ring between the base of the prism and a substrate. The laser beam enters the prism and refracts towards the base of the prism where it reflects from the prism-sample interface as indicated in Fig. 3. The reflected beam exits the prism and is refracted towards a Si photodetector. In order to characterize the reflectance as a function of the incidence angle θ_i, the prism is mounted on top of a high precision goniometer. The index of refraction of the prism at this wavelength is n_1 = 1.515. The Dove prism geometry is appropriate to measure the reflectance about the critical angle of a glass-water interface, where the contribution of the particles to the coherent reflectance is expected to be largest. To obtain the value of the reflectance at the prism-sample interface we had to correct for the Fresnel transmittance at the entrance and exit faces of the prism. The reflectance curves were taken by rotating the goniometer in steps of one degree and displacing the photodetector in synchrony to capture the reflected beam. The angle of incidence at the base of the prism θ_i, was calculated using Snell's law and the angle of entrance at the facet of the prism. Finally the system was tested and calibrated using distilled water as a reference. The accuracy on the angle of incidence in our experiments was estimated to be about 20 arc min, while the error in the reflectance was less than 1%

Before each experiment the base of the prism was carefully cleaned with distilled water, ethanol and acetone. Such a procedure was important to avoid the adsorption of the colloidal particles on the prism and obtain reproducible results First, a reflectance curve around the critical angle with distilled water was taken as a reference. At the wavelength of our laser, the refractive index of distilled water at room temperature is about n_m = 1.3313. Then, the water was replaced by the colloidal sample and a reflectance curve was taken over the same angular range. All reflectance curves were normalized with respect to the reflection signal of distilled water just after the critical angle. It was verified that, with our experimental setup, the contribution of the diffuse component in the specular direction was negligible in all the cases studied. We performed measurements with two types of particles: (i) spherical latex particles made of a blend of two polymers (Butil-poliacrylate and Metil-metacrylate) and (ii) irregularly shaped TiO_2 particles (rutile), both dispersed in water.

#8123 - $15.00 USD Received 15 July 2005; revised 15 August 2005; accepted 16 August 2005

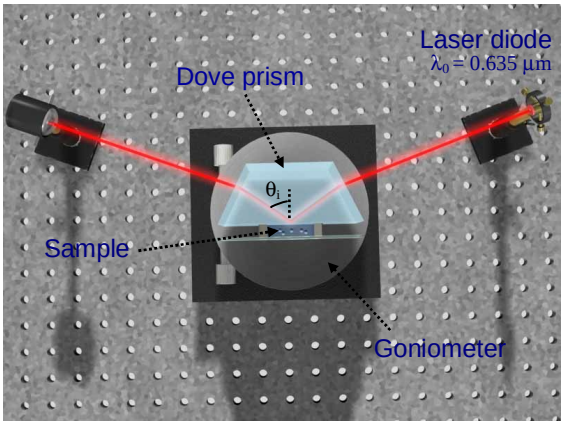

Fig.3. Schematic of the experimental setup.

The suspensions of latex particles used in our experiments were prepared by diluting with distilled water highly concentrated samples provided by the Center for Polymer Research (CIP, México). The refractive index of the particles, n_p, was expected to be between 1.47-1.48; we performed experiments with two particle sizes: $a \cong 125$ nm and $a \cong 186$ nm. The size distribution of the latex particles was determined by dynamic light scattering using a commercial apparatus. It was found that the particles had a narrow size distribution with a polydispersity index of about 1.04, thus, the samples were considered to be monodisperse in the theoretical calculations.

The suspensions of TiO_2 particles were prepared by dispersing dry TiO_2 powder in distilled water. To reduce the formation of aggregates we added a surfactant and placed the suspensions 5 minutes in an ultrasonic bath before measurements were done. However, not all powder could be dispersed and a portion of it remained clogged at the bottom of the sample container. Therefore, we did no have an accurate estimation of the particle density of the suspensions prepared. The refractive index of the particles is assumed to be $n_p \approx 2.73$, which corresponds to the average of the ordinary and extraordinary refractive indices of the TiO_2 in rutile phase at the wavelength of the incident radiation. A previous characterization of the particles by electron microscopy [26] showed that their shape was irregular but most crystallites had a spheroidal shape with a wide size distribution. The size distribution followed a log-normal distribution with estimated values of σ and a_0 of about 1.33 and 112.5 nm, respectively. A possible source of errors is that TiO_2 particles suspended in water will sediment over time since the relative density of TiO_2 is about 4. However, we checked for differences between reflectance data of TiO_2 suspensions taken half an hour apart and found that they were small (less than about 2%). On the other hand, measuring a reflectance curve in our experiments took about 5 minutes. Therefore, the reflectance data taken in one experiment with a TiO_2 suspension may be considered safely to be for the same value of the volume filling fraction.

4. Results

4.1. Results for latex particles

In Fig. 4 we show experimental data of the reflectance of TE polarized light for latex particles of radius of about 125 nm. Four graphs for different values of the volume filling fraction, f = 2.75%, 4.9%, 6.4% and 14.0% are shown. We include in the figure curves calculated with the coherent-scattering model (CSM) and the isotropic effective-medium model (IEMM). The values of a, f, n_m, and n_p used for the theoretical curves were adjusted to fit best the experimental data. In this case we did not have an accurate estimation of the volume fraction of the samples because, as it was later realized, the polymerization reaction used to fabricate the particles was not complete. This means that we could not estimate the number density of

#8123 - $15.00 USD Received 15 July 2005; revised 15 August 2005; accepted 16 August 2005

particles in suspension from the amount of the materials used to prepare the original samples and from the particle size determined by dynamic light scattering measurements. Also, the refractive index of the matrix could be somewhat larger than that of pure water due to the unknown amount of monomers left dissolved in the water. Therefore, we searched for the value of the volume fraction over a large range while keeping the values of a and n_p close to their nominal values to fit the experimental data. We also increased slightly the value of the refractive index of the water.

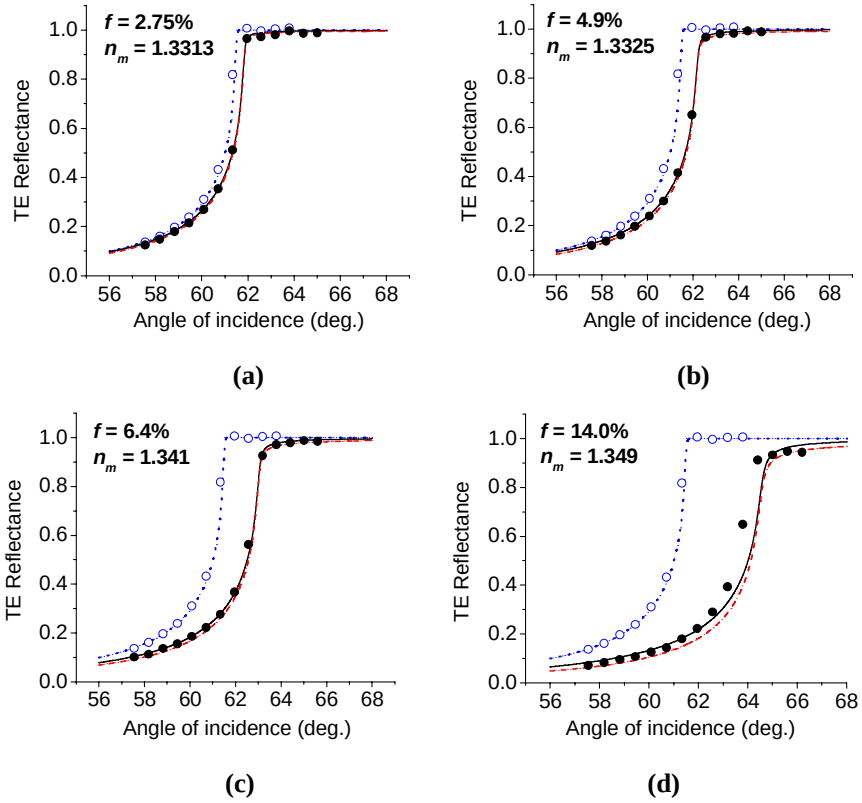

Fig. 4. Reflectance results for a TE polarization using a suspension of latex particles. Experimental data for ○ water and ● particle suspension. Theoretical curves are calculated with: n_p=1.48, n_m=1.3313, a =120.5 nm,. (a) f = 2.75 %, (b) f = 4.9 %, (c) f = 6.4 %, and (d) f = 14.0%, for —— CSM, ----- IEMM and ····· pure water.

We can appreciate in Fig. 4 that the CSM as well as the IEMM reproduce fairly well the experimental data for volume fractions f = 2.75%, 4.9%, and 6.4%. The value of the particles radii adjusted for the theoretical curves agrees well with the average particle size determined by dynamic light scattering and the refractive index of the particles is within the interval expected. For a larger value of f, of about 14%, neither model can reproduce the experimental data. Therefore these results support the validity of both models for values of f up to 6.4% and a particle radius of about 120 nm.

#8123 - $15.00 USD Received 15 July 2005; revised 15 August 2005; accepted 16 August 2005

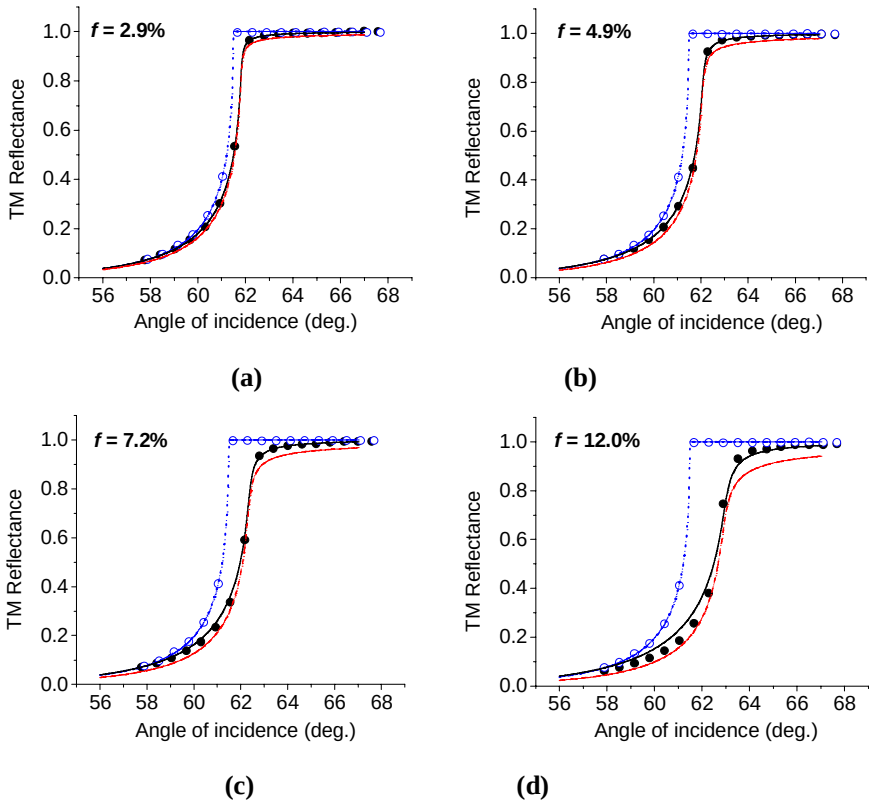

Fig. 5. Reflectance results for a TM polarization using a suspension of latex particles. Experimental data for ○ water and ● particle suspension. Theoretical curves are calculated with: n_p=1.47, n_m=1.3313, a =186.5 nm. (a) f = 2.9 %, (b) f = 4.9 %, (c) f = 7.2 %, and (d) f = 12.0%, for —— CSM, ----- IEMM and ····· pure water.

In Figure 5 we present our results for latex particles with a diameter of about 186 nm. For these experiments the light polarization was TM. We also show four graphs for different values of the volume fraction between 2.9% and 12.0%. In this case we had a fair estimation of the volume fractions in the samples prepared for the experiments because the polymerization reaction that formed the particles was complete. The nominal values of f were f_{nom} = 3%, 5%, 7% and 12% with a relative uncertainty of about 5%. The adjusted values shown in the inset of the graphs are f = 2.9%, 4.9%, 7.2% and 12% which coincide with the nominal values within the uncertainty. The particles radius used to adjust the CSM to the experimental data coincides with that obtained by dynamic light scattering measurements. The refractive index of the particles in the adjusted curves is n_p = 1.47 which also lies within the expected range. After finalizing the experiments we filtered the particles out from one sample and measured the refractive index of the remaining water. Its value differed at most by 3 units in the fourth digit from that of pure water. This means that there was a negligible amount of monomer dissolved in the water and one should expect the agreement between the nominal values of f and those used to adjust the theoretical curves.

We also performed measurements of the average extinction cross section of the particles by transmission through a 1 mm thick glass container filled with diluted samples. The obtained cross section was consistent with the adjusted values in Fig. 5. We can appreciate that the CSM reproduces very well the experimental data for f = 2.9%, 4.9% and it still does fairly well for f = 7.2%. For f = 12% the CSM deviates noticeably from the experimental data. For f = 2.9%, 4.9% and 7.2% we see that the IEMM is somewhat off the experimental data and further off for f = 12%. In this experiment, we had a fair knowledge of the value of all the

#8123 - $15.00 USD Received 15 July 2005; revised 15 August 2005; accepted 16 August 2005

parameters required in the reflectance model and we see that all the adjusted values coincide with them. Therefore, this experiment gives clear evidence of the validity of the CSM and of the limitations of the IEMM to model large particles.

4.2. Results for TiO_2 particles

We obtained similar results of the coherent reflectance as a function of the angle of incidence for suspensions of TiO_2 particles in water. In these experiments the volume filling fractions used were much lower than for latex particles since TiO_2 particles disperse light a lot more efficiently. In Fig. 6 we present three graphs for three different values of f : 0.38%, 0.70% and 1.20%. In this case the polarization of light was TE and we compare the experimental data with results from CSM and IEMM for polydispersed systems assuming a log-normal size distribution. We varied the values of f, σ, and a_0 to fit the experimental data and used the nominal values for the refractive index of the particles and water, namely, $n_p = 2.73$ and $n_m = 1.3313$. The adjusted value of a_0 is 126.6 nm and differs less than 13% from the value estimated by electron microscopy. The values of f were varied over a large range since we did not have an accurate estimation of the volume fraction. The reason is that not all the particles could be dispersed when preparing the particle suspensions and some remained clogged at the bottom of the container where the samples were prepared. The value of σ used for the theoretical curves, 1.23, differs from that estimated by electron microscopy, 1.33. Using a larger value of σ deteriorates the fitting. A possible reason of this discrepancy is that larger particles sediment faster than smaller ones and, after time passes, the width of the size distribution of particles suspended in water decreases. Nevertheless, in the log-normal distribution the difference between a value of $\sigma = 1.23$ and $\sigma = 1.33$ is not large. We again see that the CSM reproduces fairly well the experimental data, while the IEMM does not. In this case the differences of both models are larger. Actually, trying to fit the IEMM to the experimental data was unsuccessful, even for the experiment with the smallest value of f.

In Fig. 7 we show similar curves but for TM polarization. The samples used in these experiments were prepared from a different lot of particles, presumably with the same characteristics. We show graphs only for two different values of f. To fit the CSM model we again supposed the nominal values of $n_p = 2.73$ and $n_m = 1.3313$. We varied the values of f, σ, and a_0 to fit the experimental data of the two experiments consistently. In this case the value of a_0 found is 107.6 nm and differs less than 5% from the estimated value by electron microscopy. We again found that a somewhat smaller width of the size distribution, $\sigma = 1.23$, fitted better the experimental data. Here the CSM reproduces again well the experimental data while the IEMM could not be fitted and the differences with the CSM are important all along the angular range shown. In this experiment we also performed measurements of the average extinction cross section of the particles. Again, we did this by transmission through a 1 mm thick glass container filled with diluted samples, and found that the measured cross section was consistent with the values of n_p, n_m, f, σ, and a_0 used in Fig. 7. The second graph in Fig. 7 is for an adjusted value of $f = 2.1\%$. Note that the change in reflectance behind the critical angle with water is about 75%. Similarly, in Fig. 5 for latex particles we can appreciate changes up to 80%. These changes in reflectance about the critical angle are quite strong and allow us to detect the presence of the particles in suspension easily, even though the particle suspension is in the diluted regime. In this sense testing the CSM in an internal reflection configuration and about the critical angle provides stronger evidence of its validity.

#8123 - $15.00 USD Received 15 July 2005; revised 15 August 2005; accepted 16 August 2005

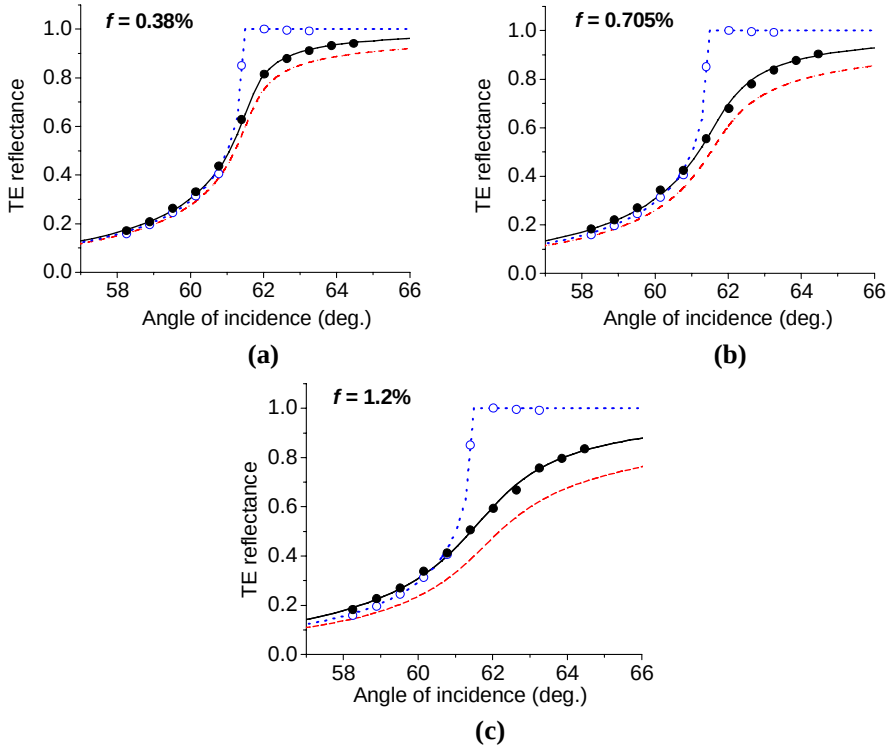

Fig. 6. Reflectance results for a TE polarization using a suspension of TiO_2 particles. Experimental data for ○ water and ● particle suspension. Theoretical curves are calculated with: n_p=2.73, n_m=1.3313, a_o=126.6 nm, σ=1.23, a) f = 0.38 %, b) f = 0.705 % and c) f = 1.2 %, for —— CSM, -----IEMM and ····· pure water.

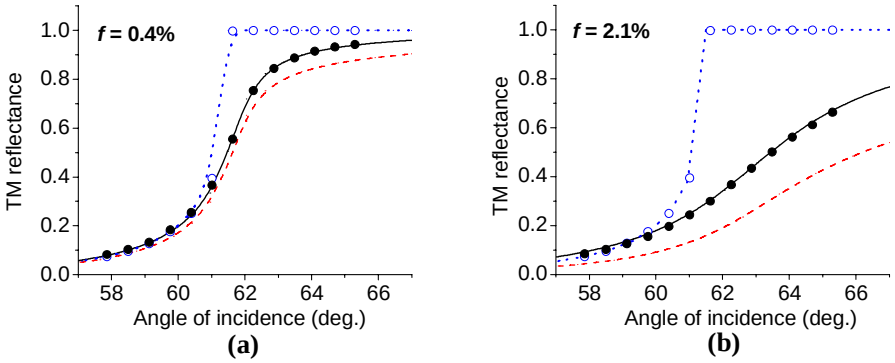

Fig.7. Reflectance results for a TM polarization using a suspension of TiO_2 particles. Experimental data for ○ water and ● particle suspension. Theoretical curves are calculated with: n_p=2.73, n_m=1.3313, a_o=107.6 nm, σ = 1.23, a) f = 0.4 %, and b) f = 2.1 %, for —— CSM, ----- IEMM and ····· pure water.

5. Conclusions

In this work we presented a comparison of our own measurements of the reflectance of light from a dilute random system of particles embedded in a boundless, non-absorbing, homogeneous matrix, with the predictions of a coherent-scattering model. Experiments were performed in an internal-reflection configuration and near the critical angle, where the

#8123 - $15.00 USD Received 15 July 2005; revised 15 August 2005; accepted 16 August 2005

contribution of the particles to the reflectance is expected to be largest. We also introduced the isotropic effective-medium model as a naïve application of the Fresnel's relations and the effective-medium concept. The experiments were performed with diluted suspensions of latex and TiO_2 (rutile) particles in water. We obtained reflectance data about the critical angle defined by the glass-water interface. The suspensions of latex particles used in this work had a narrow size distribution and were considered monodisperse; whereas the TiO_2 suspensions had a wide particle size distribution following a log-normal distribution. We then compared the coherent-scattering model and the isotropic effective-medium model to experimental data.

We found that the coherent-scattering model could reproduce fairly well the experimental data within the experimental uncertainty; whereas the isotropic effective medium model could not. Therefore, the experimental results support the validity of the coherent-scattering model and confirm that Fresnel relations are not satisfied with a colloidal medium when the size parameter of the particles is not small, and the medium is, in consequence, turbid. Although our results are not exhaustive, they definitely support the validity of the coherent-scattering model for dilute suspensions with a volume fraction up to the order of a few percent and for particles with a refractive index as high as 2.7. Even though the coherent-scattering model presented here is limited to dilute suspensions, it was able to reproduce accurately changes in reflectance as high as 80%, when the measurements are performed close to the critical angle.

Theory and experiments show that in an internal-reflection configuration about the critical angle, there is a high sensitivity of the optical reflectance to changes in particle concentration and the type of particles in suspension. In a critical-angle refractometer, the effective refractive index of the external media is obtained by using the isotropic effective-medium model. This is usually done by determining the angular location of the inflexion point of the reflectance curve about the critical angle. The Fresnel's reflection coefficients relate in a simple way the effective refractive index to the inflexion point. However, the relation between the coherent reflectance and the effective refractive index is not explicit in the coherent-scattering model as it is in the case of Fresnel's relations. Therefore, another conclusion of our work is that, in general, one cannot obtain accurately the effective refractive index of a turbid medium from a critical angle refractometer once the size parameter of the particles is large enough, since the relation between the Fresnel reflection coefficients and the effective refractive index is no longer valid. However, when the size parameter of the particles is rather small, as well as the contrast of their refractive index with respect to the one of the matrix, a critical angle refractometer may still produce accurate results, even though the colloidal suspension is already turbid. The coherent-scattering model could now be used to perform detail analysis of the errors involved in critical-angle refractometers, when applied to turbid colloids.

Nevertheless, the results presented here show that in practice, it is potentially very useful to measure the coherent reflectance about the critical angle, given its high sensitivity to the presence of colloidal particles. If one is aiming to characterize highly scattering particles, this offers a new alternative: one may invert the experimental reflectance curves about the critical angle using the coherent-scattering model, and obtain one or more of the following parameters: n_p, n_m, a_0, σ, and f. For this, it will be necessary to perform, in the near future, a sensitivity analysis of the reflectance curve to changes in these parameters.

Acknowledgments

We acknowledge financial support from Dirección General de Asuntos del Personal Académico from Universidad Nacional Autónoma de México through grants IN-108402-3 and IN-112905. We are grateful to Asur Guadarrama and Rafael Salazar for technical assistance during the experiments. We are also grateful to Arúbal Castellanos for preparing Fig. 3.

#8123 - $15.00 USD Received 15 July 2005; revised 15 August 2005; accepted 16 August 2005